frontiers | Frontiers in Marine Science

TYPE Original Research
PUBLISHED 01 October 2024
DOI 10.3389/fmars.2024.1392671

OPEN ACCESS

EDITED BY
Michelle Jillian Devlin,
Centre for Environment, Fisheries and Aquaculture Science (CEFAS), United Kingdom

REVIEWED BY
Natalya D. Gallo,
University of Bergen, Norway
Simone R. Alin,
National Oceanic and Atmospheric Administration (NOAA), United States

*CORRESPONDENCE
Christina A. Frieder
christinaf@sccwrp.org

RECEIVED 28 February 2024
ACCEPTED 22 August 2024
PUBLISHED 01 October 2024

CITATION
Frieder CA, Kessouri F, Ho M, Sutula M, Bianchi D, McWilliams JC, Deutsch C and Howard E (2024) Effects of urban eutrophication on pelagic habitat capacity in the Southern California Bight.
Front. Mar. Sci. 11:1392671.
doi: 10.3389/fmars.2024.1392671

Effects of urban eutrophication on pelagic habitat capacity in the Southern California Bight

Christina A. Frieder[1*], Fayçal Kessouri[1,2], Minna Ho[1,2], Martha Sutula[1], Daniele Bianchi[2], James C. McWilliams[2], Curtis Deutsch[3,4] and Evan Howard[5]

[1]Southern California Coastal Water Research Project, Costa Mesa, CA, United States, [2]Department of Atmospheric and Oceanic Sciences, University of California, Los Angeles, Los Angeles, CA, United States, [3]Department of Geosciences, Princeton University, Princeton, NJ, United States, [4]High Meadows Environmental Institute, Princeton University, Princeton, NJ, United States, [5]Cooperative Institute for Climate, Ocean, and Ecosystem Studies, University of Washington, Seattle, WA, United States

Land-based nutrient inputs to the ocean have been linked to increased coastal productivity, subsurface acidification and O_2 loss, even in upwelling systems like the Southern California Bight. However, whether eutrophication alters the [environment's] capacity to support key taxa has yet to be evaluated for this region. Here, we assess the impact of land-based nutrient inputs on the availability of aerobic and calcifying habitat for key pelagic taxa using ocean model simulations. We find that acute, lethal conditions are not commonly induced in epipelagic surface waters, but that sublethal, ecologically relevant changes are pervasive. Land-based nutrient inputs reduce the potential aerobic and calcifier habitat during late summer, when viable habitat is at its seasonal minimum. A region of annually recurring habitat compression is predicted 30 – 90 km from the mainland, southeast of Santa Catalina Island. Here, both aerobic and calcifier habitat is vertically compressed by, on average, 25%, but can be as much as 60%. This effect can be traced to enhanced remineralization of organic matter that originates from the coast. These findings suggest that effects of land-based nutrients are not restricted to chemistry but extend to habitat capacity for multiple taxa of ecological and economic importance. Considerable uncertainty exists, however, in how this habitat compression translates to population-level effects.

KEYWORDS

metabolic index, aerobic habitat, pteropod, anchovy, oxygen loss, ocean acidification, nutrient inputs, epipelagic

1 Introduction

Global change is fundamentally restructuring marine ecosystems, shifting distributions, phenologies, and interactions among species. Temperature (T), oxygen (O_2), and carbonate chemistry (e.g., pH, Ω_{Ar}) naturally constrain available habitat for marine calcifiers and aerobic animals, but as ocean waters warm, become less oxygenated, and more acidified, these changes are driving habitats beyond the envelope of natural variability, resulting in major

changes to species distribution and abundance, and raising the potential for major ecosystem disruptions (Howard et al., 2020; Pinsky et al., 2020). While shifts in species abundance or geographic range can be detected in historical data, local human impacts from nitrogen pollution and coastal eutrophication confound the attribution of biological changes to long-term climate trends. Effective coastal ecosystem management in the face of global change requires the means to both: (1) quantify these fundamental changes to species habitats and (2) disentangle the relative roles of climate change, natural and climatic variability, and local anthropogenic pressures in shaping those habitats. Ocean numerical models are routinely used to project the effects of climate change on shifting habitats and species distributions (Penn and Deutsch, 2022), but few coastal numerical modeling studies have investigated the potential for local coastal eutrophication to constraint marine calcifier and aerobic habitat (Bednaršek et al., 2020). As 80% of global wastewater receives no treatment before discharging to coastal waters (Rangel-Buitrago et al., 2024), such studies can help to understand whether local management of coastal eutrophication could meaningfully increase resilience of ecosystems to climate change.

In semi-enclosed seas and estuaries, the effects of eutrophication on increased primary productivity, enhanced remineralization rates, subsurface O_2 depletion, and acidification are commonly observed within the 100-m isobath (Rabalais, 2005; Rabalais et al., 2009). However, recent work has revealed that such changes can be meaningful even in upwelling-dominated coastal environments, countering the tenet that low O_2 and Ω_{Ar} that occur along eastern boundary upwelling systems are only naturally induced, without direct anthropogenic influence (Fennel and Testa, 2019). The Southern California Bight (SCB) is an open embayment situated within an eastern boundary upwelling system, located between the Baja California Peninsula and Point Conception. This region hosts a variety of marine communities and hotspots of biodiversity. The complex seabed topography and presence of islands contributes to complex circulation features. While large-scale circulation features are dominated by the California Current, submesoscale eddies accumulate and redistribute material from the coast (Dong et al., 2009). The SCB receives export from a human population of 22 million, which rivals natural upwelling in magnitude, roughly doubling available nitrogen (Howard et al., 2014). These inputs include point and non-point source discharges to the ocean from 19 ocean outfalls and 75 rivers, which release, on average, 8 million m^3 d^{-1} of nutrient-enriched water to the ocean (Sutula et al., 2021). The ocean outfalls all have wastewater treatment, but the majority have no nitrogen removal (Sutula et al., 2021). The effects of these inputs are increasing primary production and subsurface remineralization rates along the coast, with corresponding subsurface reductions in O_2 and aragonite saturation state (Ω_{Ar}) that rival or exceed that of global open-ocean O_2 loss and acidification since the pre-industrial period (Kessouri et al., 2021b).

While Kessouri et al. (2021b) quantified the change in seawater chemistry from anthropogenic nutrient inputs in the Bight, they did not document the potential for biological effects, a fundamental science gap that motivates coastal water quality managers. In the SCB, these changes in seawater chemistry can extend more than 100 km from the coast (~30% of the Bight) (Kessouri, 2024). The region of maximum change occurs in the epipelagic zone, localized between 50 and 200 m water depth. When these declines are superimposed on areas already naturally low in O_2 and Ω_{Ar}, even small changes could be of biogeochemical and ecological significance (Levin, 2018; Roman et al., 2019). The question is whether these subsurface O_2 and acidification changes are occurring at ecologically relevant conditions, resulting in vertical compression of habitat. There are field-based demonstrated consequences of coastal acidification for shell-building zooplankton, in particular pteropods (Bednaršek et al., 2019; Feely et al., 2024). Similarly, O_2 depletion in the ocean can reduce metabolic performance of aerobic taxa (Fry, 1971; Pörtner and Knust, 2007; Seibel, 2011). Most of the literature on hypoxia focuses on acute lethal levels, but sublethal effects, even subtle ones that pose constraints on feeding times, can combine to limit growth or reproduction (Gunderson and Leal, 2016; Pinsky et al., 2020). Studies in other ecosystems have documented how short-term, low-O_2 events can give rise to immediate habitat compression of sensitive species, increasing susceptibility to overfishing [e.g. of brown shrimp and demersal fishes in the Gulf of Mexico (Craig, 2012) and of artisanal fisheries species in the Sea of Oman (Piontkovski and Al-Oufi, 2014)]. Even the behavior of smaller vertical-migrating taxa, like copepods, is shaped by seasonal O_2 and temperature (Pierson et al., 2017). On the longer-term, interactions between temperature and O_2 availability on aerobic metabolism have strong correspondence with faunal diversity, species distributions, predator-prey interactions, and changing biogeographic patterns (Deutsch et al., 2015, 2020; Seibel, 2016), and may even result in range shifts (Pinsky et al., 2020; Howard et al., 2020) and extinction (Penn and Deutsch, 2022).

In this study, we assess the degree to which modeled O_2 losses and acidification due to land-based nutrient inputs translates to changes in habitat capacity. To accomplish this, we rely on two metrics that define the habitat available for aerobic metabolism and for calcification. Aerobic habitat is determined using the Metabolic Index (Φ), for which trait-based threshold varies across species. Aerobic habitat for northern anchovy, *Engrualis mordax*, is detailed but we also consider how aerobic habitat is modified for a range of species with metabolic traits that have differing oxygen and temperature sensitivities. Calcifying habitat is based on the saturation state of aragonite (Ω_{Ar}), for which thresholds also vary among species. We evaluate calcifier habitat capacity as the thickness of the water column where $\Omega_{Ar} \geq 1.4$, but we also consider the sensitivity of our results to other values of Ω_{Ar}.

Our study objectives are threefold. First, we evaluate temporal and spatial patterns in aerobic and calcifier habitat capacity metrics in the SCB with output from a 20-year numerical ocean model hindcast. Second, we test how anthropogenic nutrient inputs from land-based sources alter the vertical thickness of the habitat capacity metrics. We rely on two model scenarios, the first includes natural oceanic cycles of nutrients, O_2 and carbon, to which rising global CO_2 emissions have been imposed (referred to hereafter as 'CTRL'), and the second includes both natural oceanic cycles of nutrients and inputs from terrestrial sources, 98% of which are anthropogenic and 95% of which are point source in origin (referred to hereafter as 'ANTH') (Sutula et al., 2021). Third, we confirm the mechanisms by

which anthropogenic nutrients contribute to the observed changes in vertical habitat capacity by analyzing changes in the biogeochemical rate processes that contribute to the O_2 and carbon cycles.

2 Materials and methods

To assess whether modeled effects of land-based nutrient inputs on Bight-wide subsurface O_2 loss and acidification are biologically relevant, we employed two metrics for habitat capacity, which we adapted for this purpose. One incorporates temperature-dependent environmental O_2 as a predictor of habitat capacity for aerobic metabolism and the other incorporates carbonate chemistry as a predictor of habitat capacity for aragonite production by calcifiers. The premise of our approach is that these metrics provide information on the capacity of a specified location to provide habitat conditions that are sufficient for key processes for a species, or group of species, based on either empirical or mechanistic relationships of organismal performance with the environmental condition(s) of interest. The habitat capacity metrics are applied to model outputs from scenarios with and without land-based nutrient inputs in order to perform a difference assessment. Each metric is presented as the volume (or thickness of water-column) above a relevant threshold.

Since modeled effects of subsurface O_2 loss and acidification due to anthropogenic nutrient inputs are shown to be localized between 50 and 200 m (Kessouri, 2024), we focus our analysis on pelagic taxa. Because literature is limited on the interactive effects of O_2 and carbonate chemistry in these environments, we adapt two separate metrics to evaluate the changes in O_2 versus the changes in carbonate chemistry with an emphasis on aerobic taxa and calcifiers, accordingly.

For the effects of subsurface acidification on calcifier habitat capacity, we calculate the vertical thickness of optimal aragonite saturation state (Ω_{Ar}) conditions. A value of Ω_{Ar} of 1.4 is used to define the condition below which sublethal organismal responses have been documented to commonly occur (Bednaršek et al., 2019, 2021a, 2021b). One of the primary lines of evidence for this choice is derived from a synthesis of documented effects on pteropods (Bednaršek et al., 2019), in which Ω_{Ar} thresholds for a range of sublethal to lethal responses were identified and confidence in thresholds were judged with expert consensus. Pteropods are ubiquitous, holoplanktonic calcifiers that have a well-documented, specific sensitivity to ocean acidification. These calcifiers efficiently transfer energy from phytoplankton to higher trophic levels (Lalli and Gilmer, 1989; Hunt et al., 2008), and as such serve as an important prey group for ecologically and economically important fishes, bird, and whale diets (Armstrong et al., 2005; Aydin et al., 2005; Karpenko et al., 2007). Bednaršek et al. (2019) identified that Ω_{Ar} from 1.5 – 0.9 provides a risk range from mild dissolution to lethal impacts. Our selected value of Ω_{Ar} of 1.4 represents a value within recommended measurement precision for observational programs (± 0.2 (McLaughlin et al., 2015)) of thresholds where sublethal effects on calcification, growth, and severe dissolution are documented to occur, while a value of 1.0 roughly equates to lethal effects [0.9 to 0.95 (Bednaršek et al., 2019)]. In the epipelagic (0-200 m) in the Southern California Bight, conditions below saturation have not been common in the modern ocean (McClatchie et al., 2016), but are predicted to emerge as soon as the 2030's and 2040's (Hauri et al., 2013). However, undersaturation can occur over the benthos on the shelf (Kekuewa et al., 2022). Importantly, we perform an analysis of the sensitivity of our findings to the choice of Ω_{Ar} along this range of 1.0 to 1.4 and find the results to be largely in sensitive within this range (see Supplementary material for further details).

For the effects of subsurface O_2 loss on aerobic habitat capacity, we calculate the vertical thickness of the water column that has sufficient O_2 to provide ecological support for northern anchovy (*Engraulis mordax*). Northern anchovy is also holoplanktonic with greatest abundance observed in the upper 100 m (Mais, 1974). Defining sufficient O_2 for ecological support relies on the mechanistic framework of the Metabolic Index [Φ (Deutsch et al., 2015, 2020)]. Φ is defined as the ratio of O_2 supply to resting demand. We calculate the habitat thickness for which Phi/PhiCRIT ≥ 1; this value demarcates environment's in which anchovy can sustain active energetic demands. In contrast, values below one can sustain resting but not active energetic demands, limiting population persistence. For northern anchovy, metabolic traits have been inferred from observational datasets associated with climatological O_2 and temperature conditions (Howard et al., 2020). Similarly, we evaluate a lethal threshold for northern anchovy, where $\Phi = 1$ and O_2 supply is insufficient to meet O_2 demand. This latter analysis converts the reported active hypoxia threshold (A_o/Φ_{CRIT}) to the value at rest (A_o) using $\Phi_{CRIT} = 3.5$, the mean value across marine organisms (Deutsch et al., 2020); some species have Φ_{CRIT} as low as 1.5, in which case the lethal thresholds could occur at proportionately higher values of O_2 and thus at shallower depths.

We utilize biogeochemical output from the Regional Ocean Modeling System, ROMS (Shchepetkin and McWilliams, 2005), coupled to the Biogeochemical Elemental Cycling model, BEC (Moore et al., 2004), which has been adapted for the CCS (Deutsch et al., 2021; Renault et al., 2021). BEC is a multi-element (C, N, P, O, Fe, and Si) and multi-plankton model that includes three explicit phytoplankton functional groups (picoplankton, silicifying diatoms, and N-fixing diazotrophs), one zooplankton group, and dissolved and sinking organic detritus. Remineralization of sinking organic material follows the multi-phase mineral ballast parameterization of Armstrong et al. (2001), and sedimentary processes have also been expanded. Particulate organic matter reaching the sediment is accumulated and remineralized with a time scale of 330 days, to provide a buffer between particle deposition and nutrient release. The ecosystem is linked to a carbon system module that tracks dissolved inorganic carbon and alkalinity, and an air–sea gas exchange module based on the formulation of Wanninkhof (1992).

The SCB model domain, which extends from Tijuana Mexico to Pismo Beach (U.S. Central California coast) and about 200-km offshore, is part of a nested configuration. Model nests scale from a 4-km horizontal resolution configuration spanning the entire CCS, to a 1-km resolution grid covering much of the California coast, to a 0.3-km grid in the SCB, where our investigations of local

anthropogenic inputs were focused (Kessouri et al., 2021a, b). This grid, shown in Figure 1A, is composed of 1,400 × 600 grid points, with 60 σ-coordinate vertical levels using the stretching function described in Shchepetkin and McWilliams (Shchepetkin and McWilliams, 2005). The model is run with a time step of 30 s, and outputs are saved as 1-day averages. More information on the model setup and forcing is provided in other works (Deutsch et al., 2021; Renault et al., 2021; Kessouri et al., 2021a).

ROMS-BEC has been validated for atmospheric forcing, physics, and biogeochemistry including O_2, carbonate saturation state, primary productivity, and hydrographic parameters at a West Coast-wide scale (Deutsch et al., 2021) and, within the SCB, at scales at which anthropogenic nutrient inputs influence coastal eutrophication (Kessouri et al., 2021a).

We rely on two model scenarios. The first includes natural oceanic cycles of nutrients, carbon and oxygen cycles without terrestrial inputs (CTRL). The ocean carbon cycle includes the rising CO_2 signature from global observations. The second represents these same CTRL base conditions, to which inputs from terrestrial sources are added, 98% of which are anthropogenic and 95% of which are point source in origin (ANTH) (Sutula et al., 2021). Model simulations that include terrestrial inputs were forced with a monthly time series of spatially explicit inputs, including freshwater flow, nitrogen, phosphorus, silica, iron, and organic carbon representing natural and anthropogenic sources (Sutula et al., 2021). These data include ocean outfalls originating from Publicly Owned Treatment Works (POTW) and riverine discharges (1997–2017) and spatially explicit

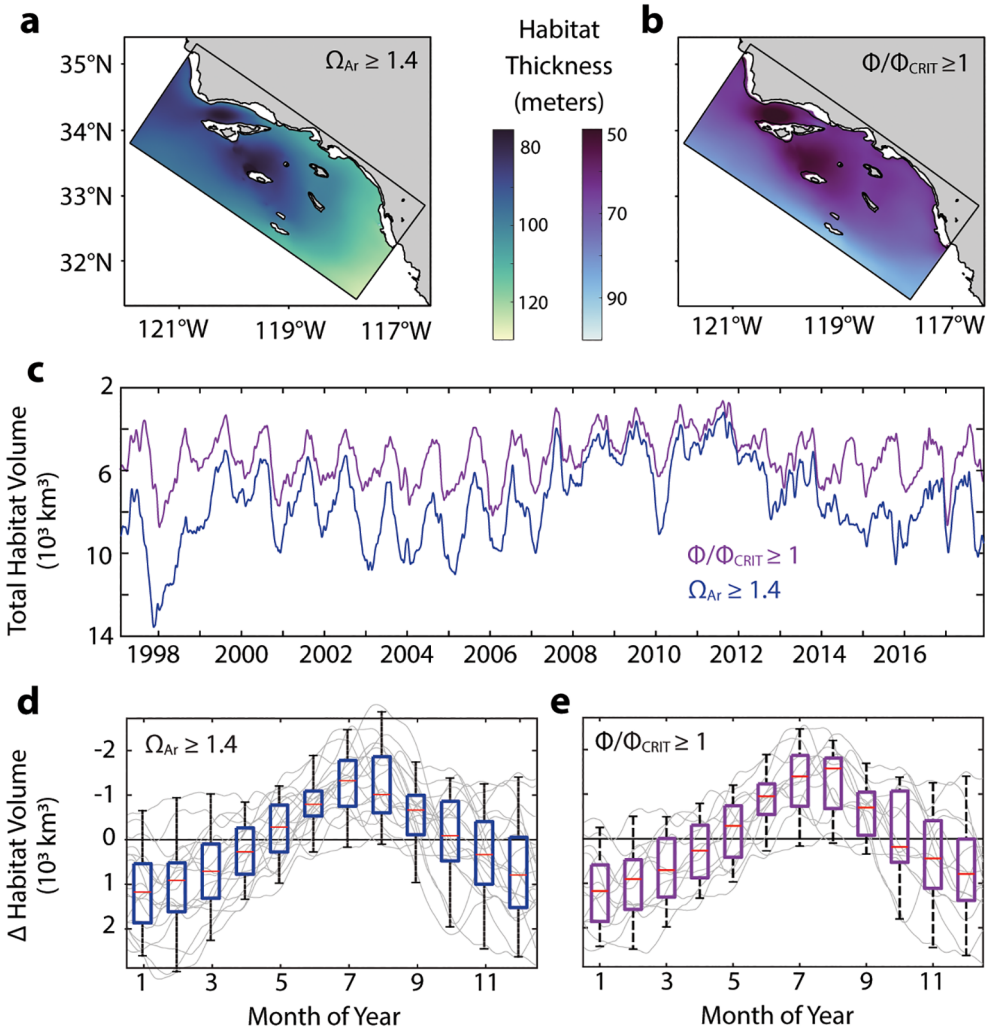

FIGURE 1
Spatial and temporal patterns in habitat thickness for aerobic and calcifier habitat metrics as assessed from model output from the ANTH scenario. **(A, B)** Spatial distribution of mean habitat thickness (m) for each biological metric. Coastline and 200-m bathymetric contours (black) shown. Locations within the domain where habitat thickness interacts with seafloor not included. **(C)** Time-series of total habitat volume (10^3 km^3) summed across the model domain for (blue) and $\Phi/\Phi_{CRIT} \geq 1$ (purple). Model output is daily with a two-week running mean applied. **(D, E)** Seasonal trend in habitat volume for each biological metric. Each annual time-series is detrended with the annual mean (light grey). Box plots (median in red, 25th and 75th percentiles indicated by the bounded box, minimum and maximum as whiskers) for the average monthly values from the annually detrended time series shown (n = 18 years). Y-axes are oriented so that a decrease in habitat volume is upwards and an increase in habitat volume is downwards.

modeled estimates of atmospheric deposition. POTW effluent data were compiled from permit monitoring databases and communication with sanitary agencies. Monthly time series of surface water runoff from 75 rivers are derived from model simulations and monitoring data (Sutula et al., 2021). The model domain includes the U.S.-Mexico border and the simulations include not only U.S. land-based nutrient inputs but also Mexico transboundary flows from the Tijuana River watershed. The CTRL simulation covers the time periods of 02/1997 – 01/2001 and 08/2012 – 11/2017. The ANTH simulation covers the time period of 02/1997 – 11/2017. The overlapping time periods available for comparison between CTRL and ANTH represent a broad range of multi-year oceanographic conditions and climatic states.

Aragonite saturation state was computed with the CO2SYS algorithms (Lewis et al., 1998; Sharp et al., 2020) using daily averages of model output fields of dissolved inorganic carbon (DIC), total alkalinity (TA), temperature, salinity, and pressure. Calcifier habitat thickness was calculated as the thickness of the water column for each grid cell that was ≥ optimal Ω_{Ar} (1.4) for pteropods.

The ecological Metabolic Index (Φ/Φ_{CRIT}) was computed from daily averages of model output fields of O_2 and temperature.

$$\frac{\Phi}{\Phi_{CRIT}} = \frac{A_o}{\Phi_{CRIT}} \times \frac{pO_2}{exp(-E_o/k_B(1/T - 1/T_{ref}))} \quad (1)$$

The metabolic traits of northern anchovy are esimated as A_o/Φ_{CRIT} = 5.4 atm^{-1} (equivalent to an active hypoxia threshold of pO_2 = 0.185 atm at 15°C) and E_o = 0.4 eV (the net temperature sensitivity of O_2 supply and demand) (Howard et al., 2020). pO_2 is the environmental partial pressure of O_2 and T is temperature (in K). k_B is the Boltzmann constant and T_{ref} is the reference temperature (here, 288.15 K). Aerobic habitat thickness was calculated as the thickness of the water column where $\Phi/\Phi_{CRIT} \geq 1$. An active hypoxia threshold of 0.185 atm O_2 at 15°C is equivalent to a saturation state of 88.5% and a concentration of 219 μmol kg^{-1} (calculated at 15°C, S=35 [pss-78], and 0 dB gauge pressure). However, we note that organismal physiology is thought to be insensitive to the concentration of oxygen. Converting the above reference value to an *in-situ* concentration requires correction for local temperature and salinity, which vary over space and time. Thus, two different concentrations could refer to the same pO_2, with no expected impact on physiological hypoxia, and vice versa.

Spatial and temporal patterns in calcifier and aerobic habitat thickness were evaluated with the ANTH simulation to identify the dominant spatial and temporal scales of variability in each. Total calcifier and aerobic habitat for the model domain was summed across all grid cells as the habitat thickness within a grid cell multiplied by the area of that grid cell.

To then evaluate how anthropogenic nutrient inputs alter calcifier and aerobic habitat thickness, we perform a difference assessment (ANTH-CTRL) where positive (negative) values represent an expansion (contraction) of habitat thickness attributable to anthropogenic nutrient inputs included in the ANTH scenario only. We focus further analyses in regions where differences in habitat thickness exceed ± 20%. We include a few sensitivity tests to some of the analytical choices. (1) To test the sensitivity of calcifier habitat capacity to the value of Ω_{Ar}, we evaluate habitat thickness for $\Omega_{Ar} \geq 1.0 - 2.5$. (2) We also calculate the change in water-column thickness for a range of $[O_2]$ from 60 – 200+ mmol m^{-3}. (3) Since northern anchovy, our species of focus for aerobic habitat, has its own temperature and oxygen sensitivity, we also explore how modeled aerobic habitat is changing for a range of temperature and oxygen sensitivities. We do this by estimating the aerobic habitat for both the ANTH and CTRL scenarios for the full combination of metabolic trait possibilities (A_o/Φ_{CRIT} and E_o). The full range of traits and their probability distribution among species have been previously compiled (Penn and Deutsch, 2022). For each metabolic trait combination, available aerobic habitat is calculated as the volume of seawater where temperature and oxygen conditions translate to an ecological Metabolic Index between 1 and 1.6 (Penn and Deutsch, 2024). The change in aerobic habitat between the scenarios is derived as the difference between ANTH and CTRL. This change is then multiplied by the probability distribution of metabolic traits across species (Supplementary Figure S1). The result is a distribution of aerobic habitat change across species. This approach assumes that the distribution of metabolic traits from the global-scale database corresponds with those in the California Current Ecosystem. We check this assumption by comparing the biogeographically inferred distribution of metabolic traits with that of respirometry-derived traits of those species found in the Southern California Bight and find that the two are indistinguishable (Supplementary Figure S1).

For regions undergoing more than a ± 20% change in habitat thickness, we evaluate the difference in the biogeochemical rate processes from each scenario [detailed methods provided in Deutsch et al. (2021) and Kessouri (2024)]. Biogeochemical rate processes that influence the O_2 cycle include surface air-sea flux, photosynthesis, non-grazing mortality, grazing mortality, water-column remineralization, sediment-water flux, NH_4 oxidation, and nitrification [Equation A9 in Deutsch et al. (2021)]. Biogeochemical rate processes that influence dissolved inorganic carbon include air-sea flux, photosynthesis, $CaCO_3$ production, non-grazing mortality, grazing mortality, and water-column and sediment remineralization [Equation A11 in Deutsch et al. (2021)]. We perform a difference assessment from the monthly averages for the sum of the biogeochemical process terms. This analysis is focused between 70 and 140-m water depth to align with the depth range where habitat thickness is affected.

3 Results

For both habitat metrics, there are consistent Bight-wide spatial and temporal patterns (Figures 1A–E), with calcifier habitat thickness greater than anchovy aerobic habitat thickness. Calcifier habitat thickness ranges from, on average, 80 to 130 m. Anchovy aerobic habitat thickness ranges, on average, from 50 to 100 m. Both habitat thickness metrics are most restricted within the Santa Barbara Channel and around San Nicolas Island. Increases generally occur along north-to-south and onshore-to-offshore gradients.

The dominant temporal scale of calcifier and anchovy aerobic habitat capacity are inter-annual and seasonal (Figures 1C–E). The temporal mean (across all years and seasons) of total calcifier and anchovy aerobic habitat volumes are 8.2 and 5.4 x 10^3 km^3, respectively, summed across the model domain. Among years, total volume for each metric can vary approximately 2-fold. In 2011, calcifier and anchovy aerobic habitat volumes were most restricted at 4.2 and 3.6 x 10^3 km^3; in 1998, habitat volumes were most expansive at 10.2 and 6.2 x 10^3 km^3, respectively. Seasonal variability also drives approximately 2-fold changes in habitat volumes. An evaluation of the annually detrended time series for both metrics shows that total habitat volumes are greatest during winter months and contract during summer, with the least amount of total habitat available during July and August (Figures 1D, E). Since anchovy aerobic habitat is constrained by both temperature and O_2, attribution analysis reveals that O_2 is the primary contributor to seasonal trends in total habitat volume, and that seasonal changes in aerobic habitat due to temperature counteract those changes due to that of O_2 (Supplementary Figure S2).

There is not a consistent tendency for land-based nutrient inputs to result in consistent or persistent Bight-wide calcifier and aerobic habitat capacity gains or losses (Supplementary Figure S3). The relative, Bight-wide differences in total habitat volume vary by ± 5% for most of the period simulated. However, at any grid cell location, the difference in calcifier habitat thickness between ANTH and CTRL can range from −34 to + 45%, and that for anchovy aerobic habitat ranges from −43 to + 80% (1st and 99th percentiles, respectively).

A spatial perspective of the change in calcifier and anchovy aerobic habitat thickness reveals a region of habitat loss that is expressed southeast of Santa Catalina Island (Supplementary Figure S3). This region of habitat loss is a seasonal phenomenon. In seven of the nine years simulated, there is a compression event lasting approximately 2.5 months that occurs in the late summer to early fall (Figures 2C, D), a time period when calcifier and anchovy aerobic habitat thickness are already seasonally compressed (Figures 1D, E). Averaging across these seven compression events, the total spatial area experiencing recurrent calcifier habitat change is 2,364 km^2 (assessed as the total spatial area where the compression in calcifier habitat thickness > 20%; Figure 2A) The equivalent total spatial area experiencing recurrent anchovy aerobic habitat change is 1,909 km^2 (Figure 2B). Despite the temporal overlap in natural seasonal and eutrophication-driven compression, there is spatial mismatch between the regions undergoing maximum habitat compression due to eutrophication with those that are naturally most restricted from broad-scale oceanographic patterns (e.g., Santa Barbara Channel; Figures 1A, B).

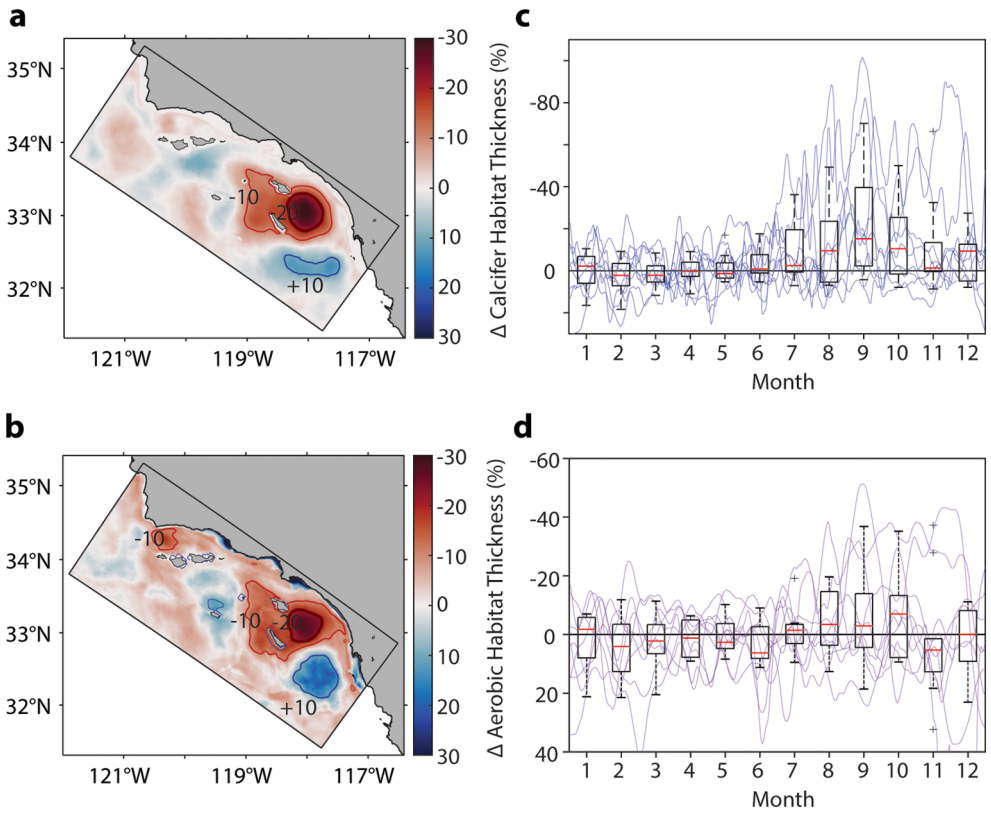

FIGURE 2
(A, B) Spatial distribution of the percent change in habitat thickness for $\Omega_{Ar} \geq 1.4$ and $\Phi/\Phi_{CRIT} \geq 1.0$ between ANTH and CTRL (from average monthly output during time periods of maximum habitat loss, n = 7 events). Thin contours show regions undergoing -10 and +10% change in habitat thickness (red and blue, respectively). Thick red contour shows region experiencing more than -20% change in habitat thickness. **(C, D)** Seasonal trend of habitat compression within the region undergoing 20% loss in habitat thickness per metric [as contoured in **(A, B)**]. Individual years (thin lines; n = 9) and box plots of mean monthly percent change in habitat thickness. Y-axes are oriented so that a compression in habitat thickness is upwards and an expansion in habitat thickness is downwards relative to zero.

Anchovy represent one ecophysiotype in a range of metabolic trait possibilities. The region of > 20% habitat compression for anchovy does not translate equally across all species (Figure 3A). In this region, ecophysiotypes with higher hypoxia tolerance (A_o/Φ_{CRIT}) gain aerobic habitat volume; while those with lower hypoxia tolerance, including anchovy, lose aerobic habitat volume. Taking a species-weighted distribution of metabolic trait possibilities, approximately two-thirds of species are losing aerobic habitat volume, and the modeled losses can be up to three times greater than the gains (Figure 3B). Of those subjected to aerobic habitat loss, 70% of species are subject to more habitat loss than northern anchovy. Species that are gaining aerobic habitat volume have higher hypoxia tolerance at any given temperature sensitivity (E_o; Figure 3A).

The spatial and vertical distribution of greatest O_2 change is occurring between approximately 40 and 100 km from the coast and between 50 and 150 meters or more below the surface (Figures 4A, C). The same pattern is observed for acidification, assessed as the difference in Ω_{Ar} between the two scenarios (Figure 4B). The lower limit of anchovy aerobic habitat coincides in space with the region of maximum O_2 loss. In the CTRL scenario, the anchovy aerobic habitat limit is at 80 m in the offshore region of maximum O_2 loss (60 km from the coast), and shoals to 60 m in the ANTH scenario. In contrast, the lower limit for calcifier habitat is deeper than the vertical region undergoing maximum acidification. Still, calcifier habitat shoals from approximately 115 m in the CTRL scenario to 87 m in the ANTH scenario. Because both subsurface acidification and O_2 loss occur across a broad depth range, our results are largely insensitive to which value of Ω_{Ar} is used to define optimal calcifier habitat (Supplementary Figure S4). Similarly, loss of O_2 is occurring across a broad depth range (Supplementary Figure S5). Notably, these changes to habitat capacity in the epipelagic are largely limited to sublethal effects as conditions that trigger acute lethal effects occur deeper in the water column. Conditions where Ω_{Ar} are less than 1 occur, on average, deeper than 200 m water depth (Supplementary Figure S4). Similarly, acute lethal O_2 conditions (Φ = 1) for northern anchovy occurs, on average, much deeper than 300 m water depth, well below the typically observed vertical distributions of anchovy and other pelagic fishes.

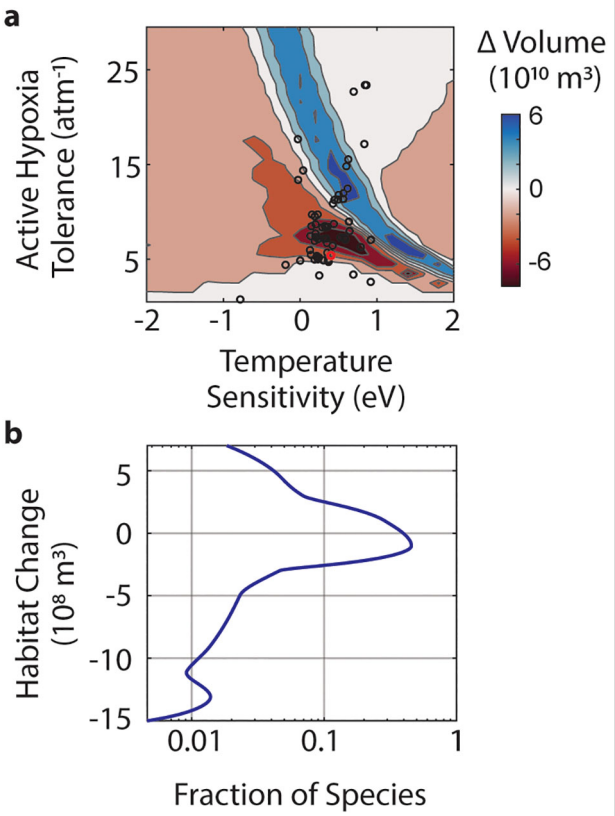

FIGURE 3
(A) Change in aerobic habitat from land-based nutrient inputs for varied marine ecophysiotypes. The range of Active Hypoxia Tolerance, A_o/Φ_{CRIT}, and temperature sensitivity, E_o, evaluated are based on a global species trait compilation; empirically derived species traits are marked with black circles, northern anchovy is marked with a red circle. Change in aerobic habitat volume assessed for the upper 200 m in the region undergoing 20% habitat compression (see Figure 2 for region of focus) from months exhibiting maximum compression in the fall (n = 7) due to land-based nutrient inputs. **(B)** Fitted distribution of the fraction of species (log scale) undergoing trait-weighted volume changes in aerobic habitat. The change in habitat volume weighted by the probability distribution of the empirical traits (Penn and Deutsch, 2022).

Of the biogeochemical rate processes contributing to habitat change within the region of 20% habitat compression, remineralization rates are exhibiting the greatest absolute change due to land-based nutrient inputs (Figure 5). For the carbon cycle, remineralization rates increase from 4.26 ± 0.12 to 4.50 ± 0.12 mmol DIC m^{-3} d^{-1} from the CTRL to the ANTH scenario (mean ± 1 SE; N = 104 months). The increase in DIC from land-based nutrient inputs at the core of habitat compression drives the modeled decrease in Ω_{Ar}. Small changes in alkalinity (< 5 mmol m^{-3}) counteract the effects due to DIC (Supplementary Figure S5). For the O_2 cycle, remineralization rates are also exhibiting the greatest change due to land-based nutrient inputs, changing from −5.44 ± 0.15 to −5.75 ± 0.15 mmol O_2 m^{-3} d^{-1} from CTRL to ANTH (mean ± 1 SE; N = 104 months).

4 Discussion

Here, we demonstrate that eutrophication effects of land-based nutrient export to the Southern California Bight are not restricted to chemical changes in seawater acidification and O_2 loss (Kessouri, 2024), but also extend to the potential for widespread (biotic and ecological) effects on calcifier and aerobic habitat capacity. The seawater chemistry changes that occur in the epipelagic are not at levels that elicit acute, lethal effects. Rather, the sublethal habitat capacity metrics used here exhibit annually recurring compression despite large, natural seasonal and interannual cycles (Figure 1). During the late summer, subsurface acidification and O_2 loss (from land-based nutrient export) routinely compress aerobic and calcifier habitat capacity (Figure 2), at a time period when habitat capacity is already seasonally compressed (Figure 1). Modeled habitat compression is most pronounced where excess nutrients and organic matter, which originate at the coast, are received and entrained within offshore eddies (Kessouri, 2024). These locations occur in both state and federal waters

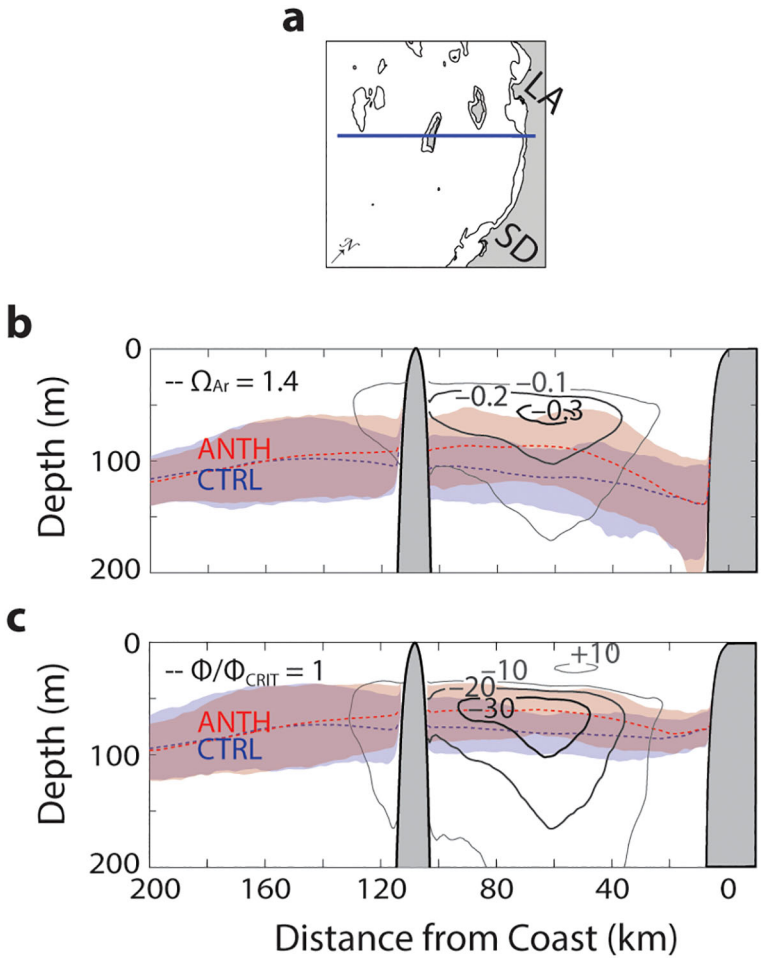

FIGURE 4
(A) Map of cross-section extending from the coast to 200 km offshore and intersected by San Nicolas Island. Coastline, Los Angeles (LA), San Diego (SD), and 200-m bathymetric contour shown. **(B)** Cross-section of mean absolute difference (contours) in Ω_{Ar} between the two simulations (ANTH-CTRL) from months exhibiting maximum compression in the fall (n = 7). The mean depth of Ω_{Ar} = 1.4 in the CTRL (blue dashed line) and ANTH (red dashed line) scenario along with 10th and 90th percentiles (shaded blue and red regions, respectively) shown. **(C)** Same as in **(B)** but contours are the absolute difference in O_2 (mmol m^{-3}) between ANTH and CTRL overlayed with the mean lower depth limit of Φ/Φ_{CRIT} = 1.

and overlap with many marine protected areas, including those around Santa Barbara Island, Santa Catalina Island, and San Clemente Island. Since seawater chemistry changes due to enhanced remineralization are occurring across a large depth range, patterns in habitat compression are largely insensitive to the value of Ω_{Ar} used to define the calcifier habitat capacity metric (Supplementary Figure S4). Similarly, while we evaluate aerobic habitat capacity for northern anchovy, we confirm that this pattern is consistent among two thirds of ecophysiotypes (although at differing magnitudes of habitat loss), and that those species gaining aerobic habitat volume have higher tolerances to low O_2 (Figure 3).

There is field-based evidence that the vertical structure of both Ω_{Ar} and O_2 have implications for a variety of pelagic taxa. For example, across frontal gradients in the California Current System where Ω_{Ar} between 1.0 and 1.4 can shoal by 100+ m on the scale of tens of kms, there are concurrent reductions in pteropod abundance accompanied by elevated shell dissolution (Bednaršek and Ohman, 2015). From onshore-to-offshore gradients, more severe pteropod shell dissolution and thinner shells occur close to the coast, particularly where upwelling is more intense (Feely et al., 2016; Mekkes et al., 2021). The predicted habitat compression described here coincides with the natural seasonal cycle of limited habitat availability. Multiple species of pteropods, including *Limacina helicina*, are present year-round in the SCB (K. McLaughlin, pers. comm.). While limited baseline information on pteropod life history characteristics exist for the Southern California Bight (Manno et al., 2017), studies suggested that spring (April-May) and fall (September-October) are periods when early life stage cohorts are most vulnerable to changing ocean conditions (Gannefors et al., 2005; Wang, 2014; Wang et al., 2017).

Ocean O_2 depletion adversely impacts marine species, assemblages, and even fisheries (Laffoley and Baxter, 2019). Long-term deoxygenation trends play a role in, for example, declines in abundance of mesopelagic fishes (Koslow et al., 2011) and shifts in zooplankton and small nekton diel migration depth (Bianchi et al., 2013). Interactive effects of sub-optimal O_2 and temperature are becoming increasingly considered (Roman et al., 2019). Sub-optimal O_2 stress depends on the O_2 supply relative to metabolic demand, and water temperature controls both chemical (O_2

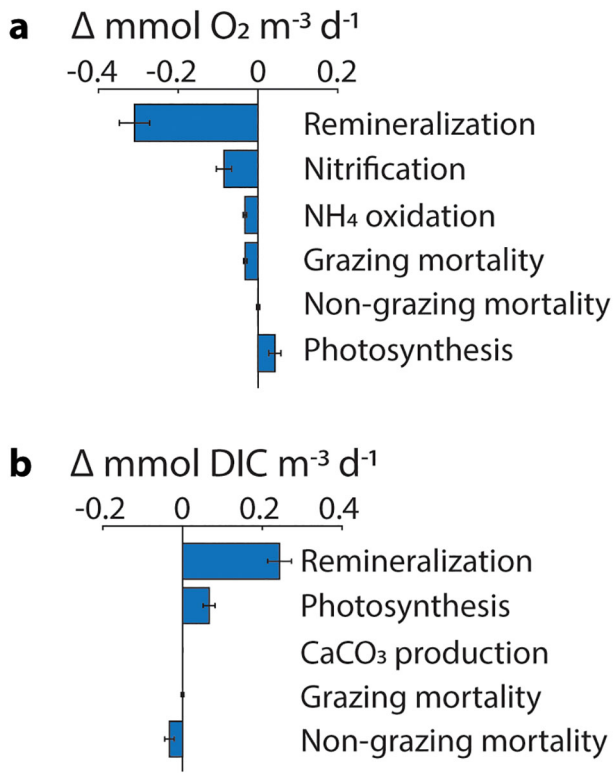

FIGURE 5
Absolute difference in the biogeochemical rate processes that contribute to the **(A)** O_2 and **(B)** dissolved inorganic C (DIC) cycles between the ANTH and CTRL scenarios. Rates are monthly averages from within the region of 20% habitat compression (Figure 2A) averaged from 70 to 140-m water depth (n = 104 months; mean ± 1 SE).

solubility, diffusivity) and physiological processes (metabolic demand, ventilations rates) affecting this balance for marine ectotherms. We use the mechanistic framework of the Metabolic Index (Deutsch et al., 2015) to incorporate these dependencies into the index of aerobic habitat capacity. Specific to our focal taxa, northern anchovy have seasonal to interdecadal redistributions that correlate with aerobic habitat capacity. For example, anchovy migrate offshore during peak upwelling seasons (Mais, 1974; Laroche and Richardson, 1980), when nearshore aerobic habitat availability is lowest, even though their food supply is generally higher closer to the coast (Howard et al., 2020). Further, the southern biogeographic limit of this species is coincident with the aerobic habitat capacity threshold implied by their oscillations in time within the SCB, and vice versa (Howard et al., 2020). While reductions in this index are associated with species-specific consequences of deoxygenation at the regional scale, it remains unclear how the spatial and seasonal extent of the O_2 reduction identified here might translate to disruptions across species of varying phenologies, mobility, and ecological niches. The same can be said for the population-level consequences of subsurface acidification.

We evaluate O_2 loss and acidification effects on habitat capacity separately, as the combined effects of these stressors on biological responses are insufficiently understood (Bednaršek et al., 2020). However, studies suggest that exposure to suboptimal ranges of acidification, O_2, and temperature can make marine organisms more sensitive to O_2 loss (Breitburg et al., 2019) or less resilient to acidification (Stevens and Gobler, 2018). In this model domain, there is strong covariance between calcifier and aerobic habitat thickness (Pearson correlation coefficient = 0.79), linked to eutrophication effects on water-column remineralization, such that aerobic and calcifier habitat compress at the same time. Thus, predicted effects on habitat capacity for marine species may be underestimated (Bednaršek et al., 2020). The Metabolic Index framework does incorporate the combined effects of temperature and O_2. Biological sensitivities to all three variables – temperature, O_2, and carbonate system state – could potentially be merged through a fundamental physiological trait such as aerobic scope [i.e., a proxy for the surplus energy available for growth, reproduction, predator avoidance, etc.; en sensu Sokolova (2021)].

While we emphasize subsurface losses in pelagic habitat capacity, changes to subsurface biogeochemistry will also intersect with the complex seafloor topography of the Southern California Bight. We have yet to evaluate how anthropogenic nutrient loads are altering habitat availability for demersal organisms, particularly those that have limited mobility. Another consideration to be further explored is the enhanced productivity and food supply from anthropogenic nutrient loads. Increased food supply could potentially reduce the negative consequences of suboptimal O_2 and acidification (Breitburg et al., 2009; de Mutsert et al., 2016). As an example, total fisheries landings can remain high even if demersal species in O_2- depleted areas decline, because nutrients can stimulate prey production in other well-mixed parts of a system (Breitburg et al., 2009; Nixon and Buckley, 2002). Abundant prey can improve stress tolerance of organisms (Marigomez et al., 2017). However, system-wide compensation through enhanced productivity will have limits as the volume of O_2- depleted waters expand (Breitburg, 2002). The catch per unit effort for selected demersal fish species along the U.S. West Coast is positively related to near-bottom O_2 concentrations, with the catch per unit effort decreasing more significantly as O_2 concentrations decrease (Keller et al., 2015). In the Humboldt Current, it is suggested that low O_2 near the coast results in a highly efficient trophic transfer and a dense anchovy population (Bertrand et al., 2011), which is beneficial for fishing activities. During these conditions, species that are less tolerant to low O_2, like sardine and jack mackerel, are restricted to offshore, well-oxygenated waters (Alegre et al., 2015; Bertrand et al., 2016).

Global climate change will further exacerbate habitat loss resulting from land-based nutrient inputs (Kessouri et al., 2021b). Strengthened stratification, from increased surface water temperatures as the global climate warms, is sufficient to worsen subsurface O_2 and acidification where it currently exists and may instigate habitat loss elsewhere (Long et al., 2019). Warming and O_2 loss by 2100 are projected to result in complete loss of aerobic habitat for northern anchovy – and thus likely extirpation – from the southern California Current System (CCS) (Howard et al., 2020). Further, the interplay of anthropogenic nutrient export and stratification where they occur could accelerate the timeline of habitat compression and potential extirpation. In this study, O_2 loss in the core of habitat compression exceeds 30 μmol kg^{-1}

(Figure 4C). This loss due to eutrophication is 1.5 times the scale of decadal O_2 loss in the southern CCS which may be occurring at around 20 μmol kg^{-1} $decade^{-1}$ (Bograd et al., 2008). Acidification in the same eutrophication-induced core exceeds −0.3 units for Ω_{Ar}, and this decrease due to eutrophication is three times the decadal trend of approximately −0.1 $decade^{-1}$ (Leinweber and Gruber, 2013; Turi et al., 2016).

To conclude, we assess change in habitat capacity for pelagic calcifying and aerobic taxa due to eutrophication effects on subsurface acidification and O_2 loss from land-based nutrients. Our findings suggest that effects of land-based nutrients are not restricted to chemistry. Changes to habitat capacity defined by sublethal, ecologically relevant thresholds were pervasive during late summer, when habitat capacity is at its seasonal minimum. Despite the theoretical, experimental, and field evidence that identify the importance of the vertical structure of both carbonate chemistry and O_2 for marine pelagic communities, whether the modeled habitat compression shown here translate to population-level effects is uncertain. Species abundance and distributional data from existing monitoring programs, like the California Cooperative Oceanic Fisheries Investigations and the Southern California Bight Regional Monitoring Program, could be assessed through the lens of eutrophication-driven habitat compression predicted here. These same monitoring programs are developing and implementing biological metrics for acidification. Coupling region-wide modeling with experimental and field programs will be a robust foundation for study of highly urbanized coastlines.

Data availability statement

Due to size of outputs, model outputs are available from the authors upon request. Requests to access these datasets should be directed to FK, faycalk@sccwrp.org; CF, christinaf@sccwrp.org.

Author contributions

CF: Conceptualization, Formal analysis, Methodology, Visualization, Writing – original draft, Writing – review & editing. FK: Conceptualization, Formal analysis, Methodology, Writing – original draft, Writing – review & editing. MH: Methodology, Writing – review & editing. MS: Conceptualization, Funding acquisition, Project administration, Writing – original draft, Writing – review & editing. DB: Conceptualization, Project administration, Writing – review & editing. JM: Conceptualization, Funding acquisition, Writing – review & editing. CD: Conceptualization, Funding acquisition, Writing – review & editing. EH: Conceptualization, Formal analysis, Visualization, Writing – review & editing.

Funding

The author(s) declare financial support was received for the research, authorship, and/or publication of this article. This research was supported by NOAA grants NA15NOS4780186, NA18NOS4780174, and NA18NOS4780167 (Coastal Hypoxia Research Program), the California Ocean Protection Council grant C0100400NSF, C0831014, and C0303000 (administered by California SeaGrant as R/OPCOAH-1), the NSF grants OCE-1419323 and OCE-1419450, and the Cooperative Institute for Climate, Ocean, & Ecosystem Studies (CICOES) under NOAA Cooperative Agreement NA20OAR4320271, Contribution No. 2024-1406. This work used the Expanse system at the San Diego Supercomputer Center through allocation TG-OCE170017 from the Advanced Cyber Infrastructure Coordination Ecosystem: Serves and Support (ACCESS) program, which is supported by National Science Foundation grants 2138259, 2138286, 2138307, 2137603, and 2138296. Additional computational resources were provided by the Hoffman2 computer cluster at the University of California Los Angeles, Institute for Digital Research and Education (IDRE). Data and code needed to run the ROMS-BEC simulations are available following the link: https://github.com/UCLA-ROMS/Code.

Conflict of interest

The authors declare that the research was conducted in the absence of any commercial or financial relationships that could be construed as a potential conflict of interest.

Publisher's note

Supplementary material

The Supplementary Material for this article can be found online at: https://www.frontiersin.org/articles/10.3389/fmars.2024.1392671/full#supplementary-material

References

Alegre, A., Bertrand, A., Espino, M., Espinoza, P., Dioses, T., Niquen, M., et al. (2015). Diet diversity of jack and chub mackerels and ecosystem changes in the northern Humboldt Current system: A long-term study. *Prog. Oceanography* 137, 299–313. doi: 10.1016/j.pocean.2015.07.010

Armstrong, J. L., Boldt, J. L., Cross, A. D., Moss, J. H., Davis, N. D., Myers, K. W., et al. (2005). Distribution, size, and interannual, seasonal and diel food habits of northern Gulf of Alaska juvenile pink salmon, *Oncorhynchus gorbuscha*. *Deep Sea Res. Part II: Topical Stud. Oceanography* 52, 247–265. doi: 10.1016/j.dsr2.2004.09.019

Armstrong, R. A., Lee, C., Hedges, J. I., Honjo, S., and Wakeham, S. G. (2001). A new, mechanistic model for organic carbon fluxes in the ocean based on the quantitative association of POC with ballast minerals. *Deep Sea Res. Part II: Topical Stud. Oceanography* 49, 219–236. doi: 10.1016/S0967-0645(01)00101-1

Aydin, K. Y., McFarlane, G. A., King, J. R., Megrey, B. A., and Myers, K. W. (2005). Linking oceanic food webs to coastal production and growth rates of Pacific salmon (*Oncorhynchus* spp.), using models on three scales. *Deep Sea Res. Part II: Topical Stud. Oceanography* 52, 757–780. doi: 10.1016/j.dsr2.2004.12.017

Bednaršek, N., Ambrose, R., Calosi, P., Childers, R. K., Feely, R. A., Litvin, S. Y., et al. (2021a). Synthesis of thresholds of ocean acidification impacts on decapods. *Front. Mar. Sci.* 8, 651102. doi: 10.3389/fmars.2021.651102

Bednaršek, N., Calosi, P., Feely, R. A., Ambrose, R., Byrne, M., Chan, K. Y. K., et al. (2021b). Synthesis of thresholds of ocean acidification impacts on echinoderms. *Front. Mar. Sci.* 8, 602601. doi: 10.3389/fmars.2021.602601

Bednaršek, N., Feely, R. A., Howes, E. L., Hunt, B. P., Kessouri, F., León, P., et al. (2019). Systematic review and meta-analysis toward synthesis of thresholds of ocean acidification impacts on calcifying pteropods and interactions with warming. *Front. Mar. Sci.* 6, 227. doi: 10.3389/fmars.2019.00227

Bednaršek, N., and Ohman, M. (2015). Changes in pteropod distributions and shell dissolution across a frontal system in the California Current System. *Mar. Ecol. Prog. Ser.* 523, 93–103. doi: 10.3354/meps11199

Bednaršek, N., Pelletier, G., Ahmed, A., and Feely, R. A. (2020). Chemical exposure due to anthropogenic ocean acidification increases risks for estuarine calcifiers in the Salish Sea: Biogeochemical model scenarios. *Front. Mar. Sci.* 7, 580. doi: 10.3389/fmars.2020.00580

Bertrand, A., Chaigneau, A., Peraltilla, S., Ledesma, J., Graco, M., Monetti, F., et al. (2011). Oxygen: a fundamental property regulating pelagic ecosystem structure in the coastal southeastern tropical Pacific. *PLoS One* 6, e29558. doi: 10.1371/journal.pone.0029558

Bertrand, A., Habasque, J., Hattab, T., Hintzen, N. T., Oliveros-Ramos, R., Gutiérrez, M., et al. (2016). 3-d habitat suitability of jack mackerel *Trachurus murphyi* in the Southeastern Pacific, a comprehensive study. *Prog. Oceanography* 146, 199–211. doi: 10.1016/j.pocean.2016.07.002

Bianchi, D., Galbraith, E. D., Carozza, D. A., Mislan, K., and Stock, C. A. (2013). Intensification of open-ocean oxygen depletion by vertically migrating animals. *Nat. Geosci.* 6, 545–548. doi: 10.1038/ngeo1837

Bograd, S. J., Castro, C. G., Di Lorenzo, E., Palacios, D. M., Bailey, H., Gilly, W., et al. (2008). Oxygen declines and the shoaling of the hypoxic boundary in the California Current. *Geophysical Res. Lett.* 35, L12607. doi: 10.1029/2008GL034185

Breitburg, D. (2002). Effects of hypoxia, and the balance between hypoxia and enrichment, on coastal fishes and fisheries. *Estuaries* 25, 767–781. doi: 10.1007/BF02804904

Breitburg, D. L., Baumann, H., Sokolova, I. M., and Frieder, C. A. (2019). "Multiple stressors–forces that combine to worsen deoxygenation and its effects," in *Ocean deoxygenation: everyone's problem. Causes, impacts, consequences and solutions*. Eds. D. Laffoley and J. M. Baxter (Gland, Switzerland: International Union for Conservation of Nature and Natural Resources).

Breitburg, D. L., Hondorp, D. W., Davias, L. A., and Diaz, R. J. (2009). Hypoxia, nitrogen, and fisheries: integrating effects across local and global landscapes. *Annu. Rev. Mar. Sci.* 1, 329–349. doi: 10.1146/annurev.marine.010908.163754

Craig, J. K. (2012). Aggregation on the edge: effects of hypoxia avoidance on the spatial distribution of brown shrimp and demersal fishes in the northern Gulf of Mexico. *Mar. Ecol. Prog. Ser.* 445, 75–95. doi: 10.3354/meps09437

de Mutsert, K., Steenbeek, J., Lewis, K., Buszowski, J., Cowan, J. H. Jr., and Christensen, V. (2016). Exploring effects of hypoxia on fish and fisheries in the northern Gulf of Mexico using a dynamic spatially explicit ecosystem model. *Ecol. Model.* 331, 142–150. doi: 10.1016/j.ecolmodel.2015.10.013

Deutsch, C., Ferrel, A., Seibel, B., Pörtner, H.-O., and Huey, R. B. (2015). Climate change tightens a metabolic constraint on marine habitats. *Science* 348, 1132–1135. doi: 10.1126/science.aaa1605

Deutsch, C., Frenzel, H., McWilliams, J. C., Renault, L., Kessouri, F., Howard, E., et al. (2021). Biogeochemical variability in the California Current System. *Prog. Oceanography* 196, 102565. doi: 10.1016/j.pocean.2021.102565

Deutsch, C., Penn, J. L., and Seibel, B. (2020). Metabolic trait diversity shapes marine biogeography. *Nature* 585, 557–562. doi: 10.1038/s41586-020-2721-y

Dong, C., Idica, E. Y., and McWilliams, J. C. (2009). Circulation and multiple-scale variability in the Southern California Bight. *Prog. Oceanography* 82, 168–190. doi: 10.1016/j.pocean.2009.07.005

Feely, R. A., Alin, S. R., Carter, B., Bednaršek, N., Hales, B., Chan, F., et al. (2016). Chemical and biological impacts of ocean acidification along the west coast of North America. *Estuarine Coast. Shelf Sci.* 183, 260–270. doi: 10.1016/j.ecss.2016.08.043

Feely, R. A., Carter, B. R., Alin, S. R., Greeley, D., and Bednaršek, N. (2024). The combined effects of ocean acidification and respiration on habitat suitability for marine calcifiers along the west coast of North America. *J. Geophysical Research: Oceans* 129, e2023JC019892. doi: 10.1029/2023JC019892

Fennel, K., and Testa, J. M. (2019). Biogeochemical controls on coastal hypoxia. *Annu. Rev. Mar. Sci.* 11, 105–130. doi: 10.1146/annurev-marine-010318-095138

Fry, F. (1971). *The effect of environmental factors on the physiology of fish. In Environmental Relations and Behavior* Vol. 6. Eds. W. Hoar and D. Randall (New York: Academic Press), 1–98. doi: 10.1016/S1546-5098(08)60146-6

Gannefors, C., Böer, M., Kattner, G., Graeve, M., Eiane, K., Gulliksen, B., et al. (2005). The arctic sea butterfly *Limacina helicina*: lipids and life strategy. *Mar. Biol.* 147, 169–177. doi: 10.1007/s00227-004-1544-y

Gunderson, A. R., and Leal, M. (2016). A conceptual framework for understanding thermal constraints on ectotherm activity with implications for predicting responses to global change. *Ecol. Lett.* 19, 111–120. doi: 10.1111/ele.12552

Hauri, C., Gruber, N., Vogt, M., Doney, S. C., Feely, R. A., Lachkar, Z., et al. (2013). Spatiotemporal variability and long-term trends of ocean acidification in the California Current System. *Biogeosciences* 10, 193–216. doi: 10.5194/bg-10-193-2013

Howard, E. M., Penn, J. L., Frenzel, H., Seibel, B. A., Bianchi, D., Renault, L., et al. (2020). Climate-driven aerobic habitat loss in the California Current System. *Sci. Adv.* 6, eaay3188. doi: 10.1126/sciadv.aay3188

Howard, M. D., Sutula, M., Caron, D. A., Chao, Y., Farrara, J. D., Frenzel, H., et al. (2014). Anthropogenic nutrient sources rival natural sources on small scales in the coastal waters of the Southern California Bight. *Limnology Oceanography* 59, 285–297. doi: 10.4319/lo.2014.59.1.0285

Hunt, B., Pakhomov, E., Hosie, G., Siegel, V., Ward, P., and Bernard, K. (2008). Pteropods in southern ocean ecosystems. *Prog. Oceanography* 78, 193–221. doi: 10.1016/j.pocean.2008.06.001

Karpenko, V. I., Volkov, A., and Koval, M. V. (2007). Diets of pacific salmon in the Sea of Okhotsk, Bering Sea, and northwest Pacific Ocean. *N. Pac. Anadr. Fish Commun. Bull.* 4, 105–116.

Kekuewa, S. A., Courtney, T. A., Cyronak, T., and Andersson, A. J. (2022). Seasonal nearshore ocean acidification and deoxygenation in the Southern California Bight. *Sci. Rep.* 12, 17969. doi: 10.1038/s41598-022-21831-y

Keller, A. A., Ciannelli, L., Wakefield, W. W., Simon, V., Barth, J. A., and Pierce, S. D. (2015). Occurrence of demersal fishes in relation to near-bottom oxygen levels within the California Current Large Marine Ecosystem. *Fisheries Oceanography* 24, 162–176. doi: 10.1111/fog.12100

Kessouri, F. (2024). Large-scale response to urban eutrophication in the southern California Current System. *Sci. Rep.* 14 (1), 7240. doi: 10.1038/s41598-024-57626-6

Kessouri, F., McLaughlin, K., Sutula, M., Bianchi, D., Ho, M., McWilliams, J. C., et al. (2021a). Configuration and validation of an oceanic physical and biogeochemical model to investigate coastal eutrophication in the Southern California Bight. *J. Adv. Modeling Earth Syst.* 13, e2020MS002296. doi: 10.1029/2020MS002296

Kessouri, F., McWilliams, J. C., Bianchi, D., Sutula, M., Renault, L., Deutsch, C., et al. (2021b). Coastal eutrophication drives acidification, oxygen loss, and ecosystem change in a major oceanic upwelling system. *Proc. Natl. Acad. Sci.* 118, e2018856118. doi: 10.1073/pnas.2018856118

Koslow, J. A., Goericke, R., Lara-Lopez, A., and Watson, W. (2011). Impact of declining intermediate-water oxygen on deepwater fishes in the California Current. *Mar. Ecol. Prog. Ser.* 436, 207–218. doi: 10.3354/meps09270

Laffoley, D., and Baxter, J. M. (2019). *Ocean deoxygenation: Everyone's problem-Causes, impacts, consequences and solutions* (Switzerland: IUCN Gland).

Lalli, C. M., and Gilmer, R. W. (1989). *Pelagic snails: The biology of holoplanktonic gastropod mollusks* (Stanford, California: Stanford University Press).

Laroche, J. L., and Richardson, S. (1980). Reproduction of northern anchovy, *Engraulis mordax*, off Oregon and Washington. *Fish. Bull.* 78, 603–618.

Leinweber, A., and Gruber, N. (2013). Variability and trends of ocean acidification in the southern California Current System: A time series from Santa Monica Bay. *J. Geophysical Research: Oceans* 118, 3622–3633. doi: 10.1002/jgrc.20259

Levin, L. A. (2018). Manifestation, drivers, and emergence of open ocean deoxygenation. *Annu. Rev. Mar. Sci.* 10, 229–260. doi: 10.1146/annurev-marine-121916-063359

Lewis, E., Wallace, D., and Allison, L. (1998). *Program developed for CO_2 system calculations.* (Upton, NY: Tech. rep., Brookhaven National Lab., Dept. of Applied Science).

Long, M., Ito, T., and Deutsch, C. (2019). "Oxygen projections for the future," in *Ocean deoxygenation: everyone's problem. Causes, impacts, consequences and solutions*. Eds. D. Laffoley and J. M. Baxter (International Union for Conservation of Nature and Natural Resources).

Mais, K. F. (1974). Pelagic fish surveys in the California Current. *Cal. Fish Game Fish. Bull.* 162, 1–79.

Manno, C., Bednaršek, N., Tarling, G. A., Peck, V. L., Comeau, S., Adhikari, D., et al. (2017). Shelled pteropods in peril: assessing vulnerability in a high CO_2 ocean. *Earth-Science Rev.* 169, 132–145. doi: 10.1016/j.earscirev.2017.04.005

Marigomez, I., Múgica, M., Izagirre, U., and Sokolova, I. M. (2017). Chronic environmental stress enhances tolerance to seasonal gradual warming in marine mussels. *PLoS One* 12, e0174359. doi: 10.1371/journal.pone.0174359

McClatchie, S., Thompson, A. R., Alin, S. R., Siedlecki, S., Watson, W., and Bograd, S. J. (2016). The influence of Pacific Equatorial Water on fish diversity in the Southern California Current System. *J. Geophysical Research: Oceans* 121, 6121–6136. doi: 10.1002/2016JC011672

McLaughlin, K., Weisberg, S. B., Dickson, A. G., Hofmann, G. E., Newton, J. A., Aseltine-Neilson, D., et al. (2015). Core principles of the California Current Acidification Network: Linking chemistry, physics, and ecological effects. *Oceanography* 28, 160–169. doi: 10.5670/oceanog

Mekkes, L., Renema, W., Bednaršek, N., Alin, S. R., Feely, R. A., Huisman, J., et al. (2021). Pteropods make thinner shells in the upwelling region of the California Current Ecosystem. *Sci. Rep.* 11, 1731. doi: 10.1038/s41598-021-81131-9

Moore, J. K., Doney, S. C., and Lindsay, K. (2004). Upper ocean ecosystem dynamics and iron cycling in a global three-dimensional model. *Global Biogeochemical Cycles* 18, GB4028. doi: 10.1029/2004GB002220

Nixon, S. W., and Buckley, B. A. (2002). "A strikingly rich zone"—nutrient enrichment and secondary production in coastal marine ecosystems. *Estuaries* 25, 782–796. doi: 10.1007/BF02804905

Penn, J. L., and Deutsch, C. (2022). Avoiding ocean mass extinction from climate warming. *Science* 376, 524–526. doi: 10.1126/science.abe9039

Penn, J. L., and Deutsch, C. (2024). Geographical and taxonomic patterns in aerobic traits of marine ectotherms. *Philos. Trans. R. Soc. B* 379, 20220487. doi: 10.1098/rstb.2022.0487

Pierson, J. J., Slater, W.-C. L., Elliott, D., and Roman, M. R. (2017). Synergistic effects of seasonal deoxygenation and temperature truncate copepod vertical migration and distribution. *Mar. Ecol. Prog. Ser.* 575, 57–68. doi: 10.3354/meps12205

Pinsky, M. L., Selden, R. L., and Kitchel, Z. J. (2020). Climate-driven shifts in marine species ranges: Scaling from organisms to communities. *Annu. Rev. Mar. Sci.* 12, 153–179. doi: 10.1146/annurev-marine-010419-010916

Piontkovski, S. A., and Al-Oufi, H. S. (2014). Oxygen minimum zone and fish landings along the Omani shelf. *J. Fisheries Aquat. Sci.* 9, 294. doi: 10.3923/jfas.2014.294.310

Pörtner, H. O., and Knust, R. (2007). Climate change affects marine fishes through the oxygen limitation of thermal tolerance. *Science* 315, 95–97. doi: 10.1126/science.1135471

Rabalais, N. (2005). "Eutrophication," in *The Global Coastal Ocean: Multiscale Interdisciplinary Processes*, vol. 13 . Eds. A. R. Robinson and K. H. Brink (Harvard University Press, Cambridge, Massachusetts and London), 821–866.

Rabalais, N. N., Turner, R. E., Díaz, R. J., and Justić, D. (2009). Global change and eutrophication of coastal waters. *ICES J. Mar. Sci.* 66, 1528–1537. doi: 10.1093/icesjms/fsp047

Rangel-Buitrago, N., Galgani, F., and Neal, W. J. (2024). Addressing the global challenge of coastal sewage pollution. *Mar. pollut. Bull.* 201, 116232. doi: 10.1016/j.marpolbul.2024.116232

Renault, L., McWilliams, J. C., Kessouri, F., Jousse, A., Frenzel, H., Chen, R., et al. (2021). Evaluation of high-resolution atmospheric and oceanic simulations of the California Current System. *Prog. Oceanography* 195, 102564. doi: 10.1016/j.pocean.2021.102564

Roman, M. R., Brandt, S. B., Houde, E. D., and Pierson, J. J. (2019). Interactive effects of hypoxia and temperature on coastal pelagic zooplankton and fish. *Front. Mar. Sci.* 6, 139. doi: 10.3389/fmars.2019.00139

Seibel, B. A. (2011). Critical oxygen levels and metabolic suppression in oceanic oxygen minimum zones. *J. Exp. Biol.* 214, 326–336. doi: 10.1242/jeb.049171

Seibel, B. A. (2016). Cephalopod susceptibility to asphyxiation via ocean incalescence, deoxygenation, and acidification. *Physiology* 31, 418–429. doi: 10.1152/physiol.00061.2015

Sharp, J. D., Pierrot, D., Humphreys, M. P., Epitalon, J.-M., Orr, J. C., Lewis, E. R., et al. (2020). *CO2SYSv3 for MATLAB*, Dataset. Zenodo. doi: 10.5281/ZENODO.3950563

Shchepetkin, A. F., and McWilliams, J. C. (2005). The regional oceanic modeling system (ROMS): a split-explicit, free-surface, topography-following-coordinate oceanic model. *Ocean Model.* 9, 347–404. doi: 10.1016/j.ocemod.2004.08.002

Sokolova, I. (2021). Bioenergetics in environmental adaptation and stress tolerance of aquatic ectotherms: linking physiology and ecology in a multi-stressor landscape. *J. Exp. Biol.* 224, jeb236802. doi: 10.1242/jeb.236802

Stevens, A. M., and Gobler, C. J. (2018). Interactive effects of acidification, hypoxia, and thermal stress on growth, respiration, and survival of four North Atlantic bivalves. *Mar. Ecol. Prog. Ser.* 604, 143–161. doi: 10.3354/meps12725

Sutula, M., Ho, M., Sengupta, A., Kessouri, F., McLaughlin, K., McCune, K., et al. (2021). A baseline of terrestrial freshwater and nitrogen fluxes to the Southern California Bight, USA. *Mar. pollut. Bull.* 170, 112669. doi: 10.1016/j.marpolbul.2021.112669

Turi, G., Lachkar, Z., Gruber, N., and Münnich, M. (2016). Climatic modulation of recent trends in ocean acidification in the California Current System. *Environ. Res. Lett.* 11, 014007. doi: 10.1088/1748-9326/11/1/014007

Wang, K. (2014). The life cycle of the pteropod *Limacina helicina* in Rivers Inlet (British Columbia, Canada). Vancouver, British Columbia, Canada: University of British Columbia.

Wang, K., Hunt, B. P., Liang, C., Pauly, D., and Pakhomov, E. A. (2017). Reassessment of the life cycle of the pteropod *Limacina helicina* from a high resolution interannual time series in the temperate North Pacific. *ICES J. Mar. Sci.* 74, 1906–1920. doi: 10.1093/icesjms/fsx014

Wanninkhof, R. (1992). Relationship between wind speed and gas exchange over the ocean. *J. Geophysical Research: Oceans* 97, 7373–7382. doi: 10.1029/92JC00188